DE GRUYTER OPEN

*Journal of* ELECTRICAL ENGINEERING, VOL 69 (2018), NO1, 52–57

# Electric measurements of PV heterojunction structures a-SiC/c-Si

**Milan Perný*, Vladimír Šály*, František Janíček*, Miroslav Mikolášek*, Michal Váry*, Jozef Huran****

Due to the particular advantages of amorphous silicon or its alloys with carbon in comparison to conventional crystalline materials makes such a material still interesting for study. The amorphous silicon carbide may be used in a number of micro-mechanical and micro-electronics applications and also for photovoltaic energy conversion devices. Boron doped thin layers of amorphous silicon carbide, presented in this paper, were prepared due to the optimization process for preparation of heterojunction solar cell structure. DC and AC measurement and subsequent evaluation were carried out in order to comprehensively assess the electrical transport processes in the prepared a-SiC/c-Si structures. We have investigated the influence of methane content in deposition gas mixture and different electrode configuration.

K e y w o r d s: amorphous silicon carbide, thin films, solar cell, impedance spectroscopy, equivalent circuit

## 1 Introduction

Photovoltaics can be a partial solution of the problem looking for alternative energy supply. The approach to elimination of the consumption of valuable and often rare materials leads to interest on thin film solutions denoted as second or the third generation of photovoltaics. Thin film technology is the topic which often represents the deposition of thin films on a cheap, also bulky, material substrate.

Amorphous compound of silicon and carbon known as amorphous silicon carbide, alternatively with added hydrogen (a-SiC:H), are the matter of growing interest in the last time period. It is related to the electrical, optical and mechanical properties of the prepared amorphous SiC. The possible tuning of energy band gap of this type of semiconductor in the range from 1.6 eV to 2.9 eV [1] is accompanied in the change of the refractive index and absorption coefficient of final thin film layer. Both these facts are beneficial also for photovoltaic applications. The used deposition technology, *eg* PECVD technology, glow discharge technique, reactive sputtering, rf sputtering, CVD and more recently pulsed laser deposition technique (PLD) [2], and set up of the process parameters (substrate temperature, reactor pressure, suitable $CH_4/SiH_4$ flow rate in the reactor) are often critical to get required properties.

SiC was originally advantageous as extremely hard material for abrasive purposes. Silicon carbides have also found application in SiC electronics for civil nuclear industry later. An amorphous SiC material, similar to its crystalline/polycrystalline SiC counterparts, finds application in microelectronics [3], optoelectronics [4], micromechanics [5] and also increasingly in photovoltaics [6]. Silicon carbide is presented and studied as material of the future for semiconductor power device manufacturing [7, 8].

Low-temperature preparation techniques, controllability of optical properties and electrical conductivity in a wide range are major advantages. Larger mechanical strength, temperature and irradiation resistance and moisture resistance are other distinct advantages.

Amorphous SiC has unique place in microelectronics, particular in the construction of sensors [9] and micro/nano electro-mechanical systems [10]. The high radiation resistance predestines the structures with a-SiC layers for use in space solar application, where the mechanical and temperature resistance is particularly required.

One of the very interesting applications of thin film of a-SiC is its use as an emitter part of heterojunction (HJ) solar cell together with crystalline silicon [11]. Greater short-circuit current and open circuit voltage are the main advantage of a-SiC compared to amorphous silicon [12]. Efficiency around 22 % of HJ solar cell was achieved by structural refinements [13]. The amorphous silicon carbide is also used as the intrinsic layer in the construction of the tandem amorphous silicon cells [14]. Passivation layers [15], antireflective layers [16] and diffusion barriers [17] are other areas of application of a-SiC in today's crystalline silicon solar technology.

In our study, we present the additional results based on the previous optimization process [18]. Influence of the flow rate of methane in the PECVD reactor on the final electric properties of heterostructures, as well as the

Faculty of Electrical Engineering and Information Technologies, Slovak University of Technology, Ilkovičova 3, 812 19 Bratislava, Slovakia, vladimir.saly@stuba.sk, ** Slovak Academy of Sciences, Institute of Electrical Engineering, Dúbravská cesta 9, 841 04 Bratislava, Slovakia, jozef.huran@savba.sk

DOI: 10.1515/jee-2018–0007, Print (till 2015) ISSN 1335-3632, On-line ISSN 1339-309X 

**Table 1.** Technological details of samples preparation

| Sample | Gass 1 (sccm) $CH_4$ | Gass 2 (sccm) $SiH_4$ | Gass 3 (sccm) Ar | Gass 4 (sccm) $H_2$ | Gass 5 (sccm) $B_2H_6$ | Temperature (°C) | Pressure (Pa) | RF power (W) | Thickness (nm) | Substrate |
|---|---|---|---|---|---|---|---|---|---|---|
| BB1 | 5 | 5 | 10 | 100 | 6 | 230 | 100 | 50 | 50 | N typ, (100), 5–8 Ωcm |
| BB2 | 3 | 5 | 10 | 100 | 6 | 230 | 100 | 50 | 50 | N typ, (100), 5–8 Ωcm |

optimization of the top grid electrode has been shown by AC and DC formalism.

## 2 Experiment and results

Heterojunction solar cell structure (term structure means in our case that it is not a completed solar cell which contains all necessary arrangements, for example, anti-reflective coating or passivation) was prepared in the experiment. The plasma CVD technique with the parallel arrangement of electrodes in reactor was used for the preparation process. The thin amorphous SiC layer was grown on the substrate of N-type crystalline silicon. P-type doped SiC layer deposited on crystalline N-type silicon creates the potential barrier which results in diode behavior of prepared structure. SiC was doped by boron. The mixture 5 % $B_2H_6$ in pure $H_2$ was the doping gas. Methane added to mixture is the source of carbon influencing the properties of final alloy SiC and hydrogen passivates dangling bonds of amorphous structure. Some other details of preparation was already published in [19]. The process was set up according our previous experimental results and optimization [18]. Some details are in Table 1.

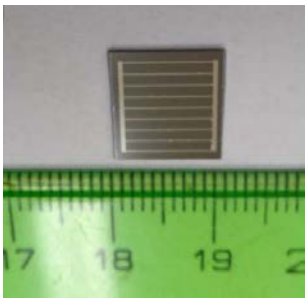


**Fig. 1.** Picture of the prepared structure

The sample area size was $0.9 \times 0.9$ cm. Samples BB1 and BB2 were produced from Al with a different density of top grid fingers. BBR with 9 lines and a BBH with 13 lines (Fig. 1). The width of fingers was 100 $\mu$m and the width of busbars on both edges was 400 $\mu$m at the thickness 200 nm. So, the active area was 66.42 mm$^2$ and 63.14 mm$^2$, resp. The whole area Al electrode is on the back. The difference between samples BB1 and BB2 is, as already mentioned, in different $CH_4$ gas flow.

Prepared samples represent the diode structure, which show the photovoltaic behavior, but principal adjustment, *eg* passivation of the surface and AR coating, is required to get better solar cell. On the other hand, prepared structures are convenient for the electrical characterization. The diode-like samples were measured in the dark and also under the illumination.

The DC measurements were performed using four-quadrant measuring source Keithley 2440 to get $I$–$V$ characteristic in the dark and under illumination. SOLARTRON Analytical Module was used for AC measurements and impedance spectroscopy technique was used for analysis of obtained data. The measurements were performed in the dark conditions at various DC bias voltage and at the frequency range from 1 Hz to 1 MHz. Impedance data were then fitted by the Eisanalyser simulation program. The irradiation source was solar simulator ORIEL which provides the radiation certified as class AAA (temporal stability, areal homogeneity and defined light spectrum).

Basic PV parameters were calculated from illuminated $I$–$V$ characteristics shown on Fig. 2.

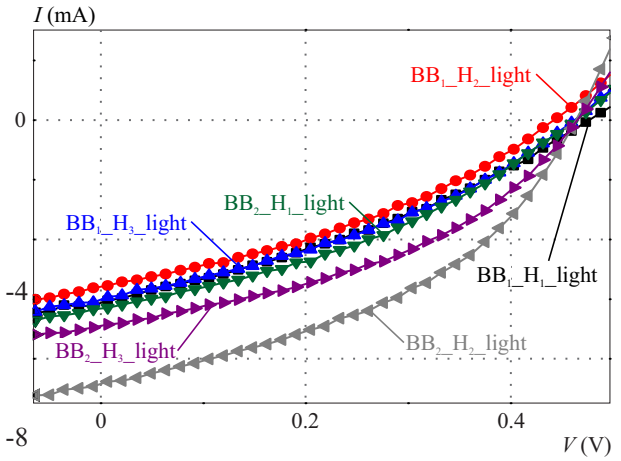


**Fig. 2.** $I$–$V$ curves obtained on various BB1, BB2 samples

The following parameters: open circuit voltage, short circuit current, maximum power point, fill factor ($FF$) and efficiency can be determined. The results obtained experimentally from the measurements under illumination

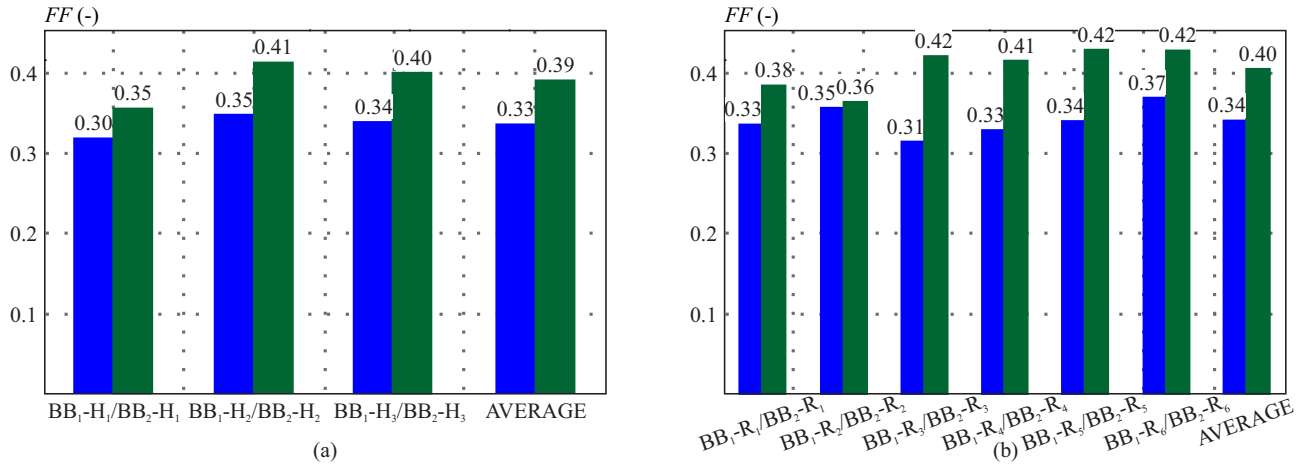


**Fig. 3.** Comparison of calculated fill factor for both BB1 and BB2 investigated series, Difference is in the electrode system configuration

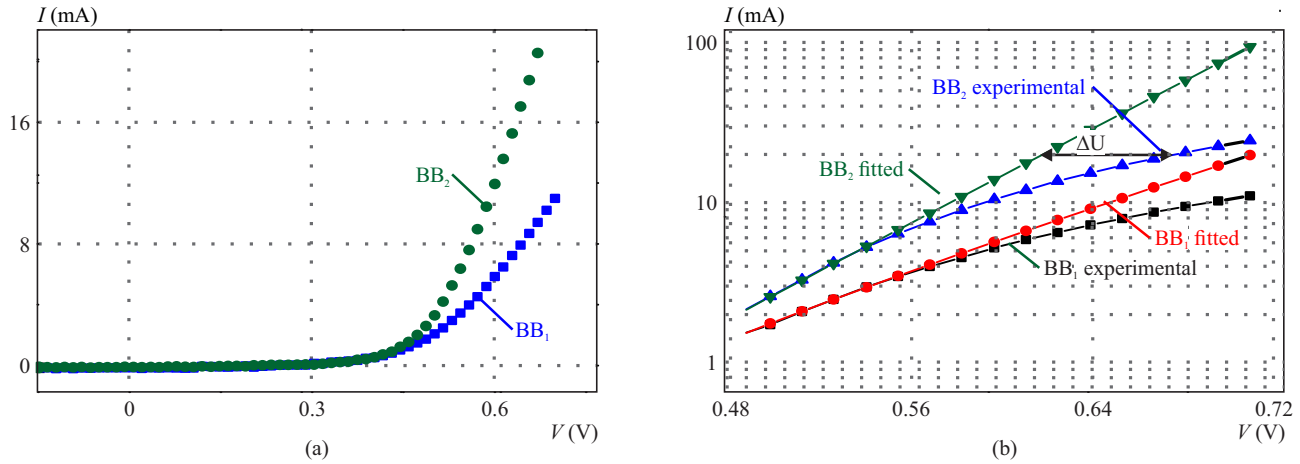


**Fig. 4.** $I$–$V$ characteristics (a) – measured in the dark for selected representative samples, and (b) – the influence of series resistance quantified by $\Delta U$ drop

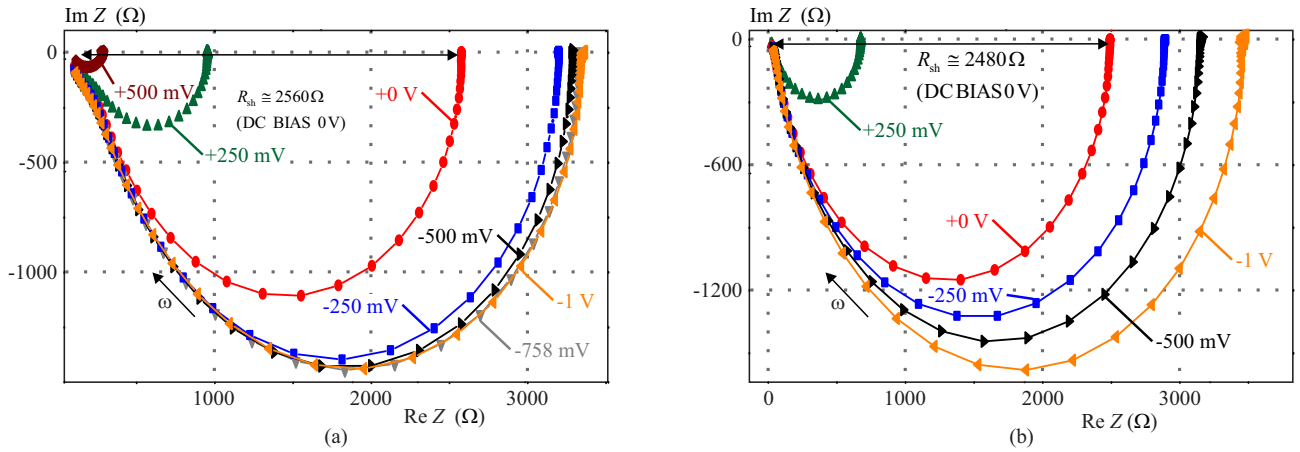


**Fig. 5.** Nyquist characteristics: (a) – for BB1-R, and (b) – for BB2-R

are illustrated in Fig. 3, where the fill factor dispersion for the both sample series with different fingers density is given. Of course, all samples show quite poor PV parameters when above mentioned optimization is missing. For the purpose of this paper, the light $I$–$V$ measurements were carried out only to compare the behavior of the prepared samples under light.

The lower concentration of precursor gas $CH_4$ during the depositions leads to better results as it is shown in Fig. 3. The value of FF 0.33 and 0.34 are lower for BB1 in comparison with the results obtained for BB2 at higher concentration of $CH_4$ – 0.39 and 0.40, resp. Similarly $I_{sc}$ and $V_{oc}$ parameters were improved.

The example of I-V curves measured in the dark are shown in Fig. 4.

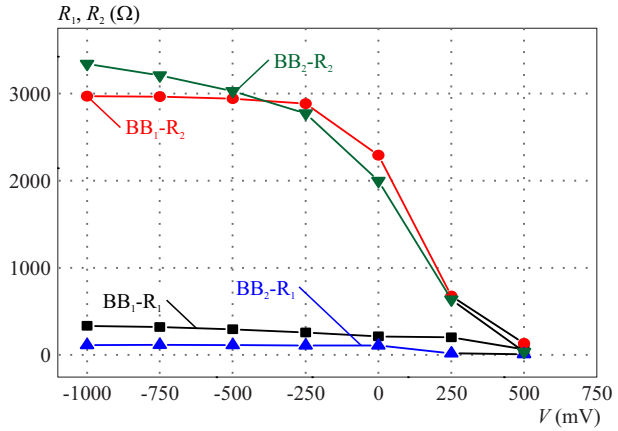


**Fig. 6.** AC equivalent resistances as a function of applied DC bias

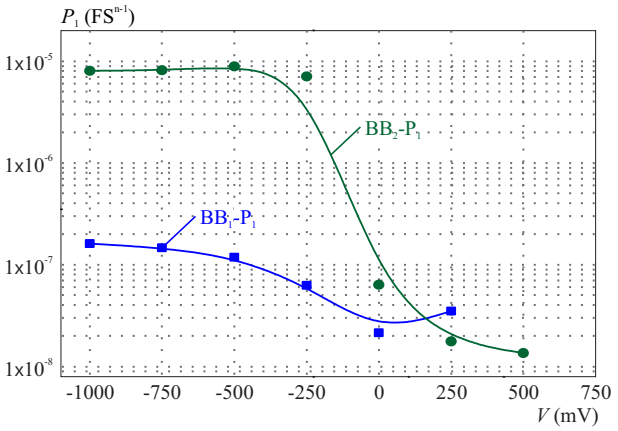


**Fig. 7.** CPE capacitance $P_1$ as a function of applied DC bias

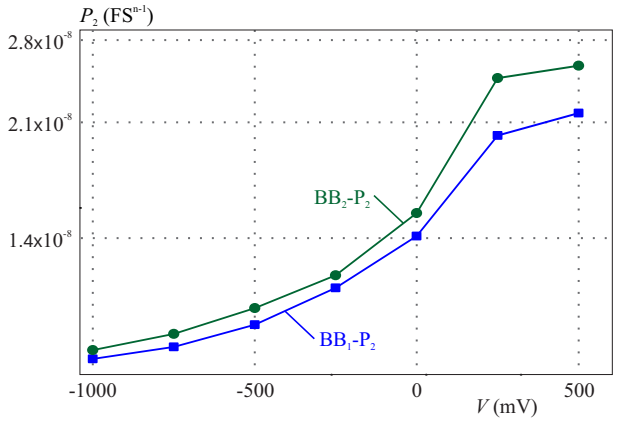


**Fig. 8.** CPE capacitance $P_2$ as a function of applied DC bias

The series resistance was calculated from the voltage drop [20] as shown in Fig. 4(b). The measured curve is compared with its linearized extrapolation. Depicted voltage drop $\Delta U$ is due to influence of $R_s$. A factor ideality of the diode was obtained using modified Shockle's equation

$$\mathrm{Ln}(I) = \mathrm{Ln}(I_0) + \frac{q}{mkT}V\,. \qquad (1)$$

The phase and absolute value of complex impedance were measured by SOLARTRON analytical module in order to obtain frequency response of SiC/c-Si heterostructure. The space charge region of PN junction varies under different DC bias, so the frequency dependence of measured impedance (Fig. 5) is modified as well when different bias is applied. AC measurements in the dark were carried out in order to identify electronic behavior. The process was based upon equivalent AC circuit, which was suggested and processed by fitting the measured impedance data. The elements like resistance, constant phase element (CPE) capacitance and CPE impedance exponent, which describe the transport processes in the structure (electronic behavior), can be extracted by standard numerical treatment based on measured AC data and proposed equivalent circuit. Individual elements of equivalent circuit and their DC voltage dependences are presented in Figs. 6–9.

AC measurements and subsequent data evaluation serve both, to determine the dynamic parameters of the structures and as the alternative to DC measurement the series resistance can be determined also and compared to the results obtained by DC measurement. The parallel/shunt resistance (limiting fill factor and efficiency) can be determined as the circle diameter of fitted experimental data, see Fig. 5.

Equivalent circuit is a simple connection of resistor $R_s$ (series resistance) in series with two parallel combinations of constant phase elements and resistors $P_1$–$R_1$ and $P_2$–$R_2$ (Fig. 10).

## 3 Discussion

Standard barrier properties of the junction were identified from measurements in the dark. The typical diode $I$–$V$ shape is in Fig. 4(a). The PV parameters $I_{\mathrm{sc}}$, $V_{\mathrm{oc}}$, $P_{\mathrm{max}}$ can be deducted from the $I$–$V$ curve under illumination and as it was already mentioned, their poor values result from the fact that well operating solar cell requires more complex structure. So the efficiency of light conversion was less than 3 % but the efficiency of BB2 was higher than that one of BB1.

The series resistance of the structure and the ideality factor were determined from the DC measurements in the dark. The series resistance, as outlined above, was determined by the numerical method from the measured $I$–$V$ dependence and the idealized straight line when $R_{\mathrm{s}} = 0\,\Omega$. Series resistance $R_{\mathrm{s}} = 4.62\,\Omega$ for BB1 and $R_{\mathrm{s}} = 1.77\,\Omega$ for BB2 was determined. The voltage drop $\Delta U$ was taken at $I = 10.98$ mA.

According (1) ideality factor $m = 3.5$ for BB1 and $m = 2.26$ for BB2. The value of the ideality factor, which is geometric factor and represents the various recombination processes in the structure, is expected to be from the range 1 to 2. For $m = 1$ it is recombination limited by minority carriers, for $m = 2$ the recombination is limited by both carrier types. However it is not unusual

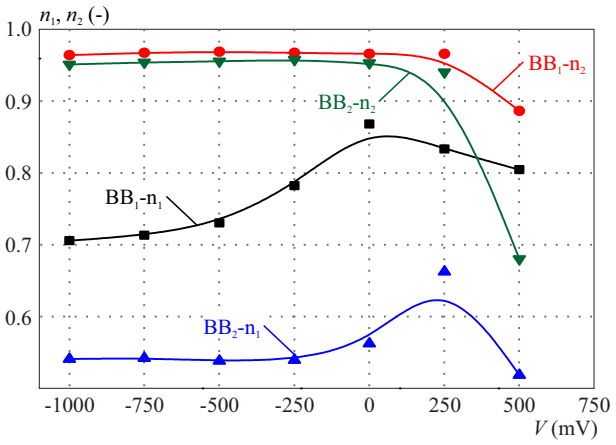


**Fig. 9.** CPE impedance exponents as a function of applied bias

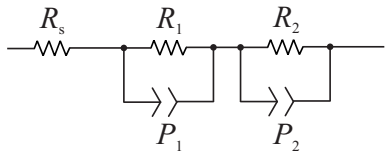


**Fig. 10.** An AC equivalent circuit of the investigated PV structures that represents individual electrical transport processes, CPE is here denoted as $P_1$, $P_2$

and known that many types of solar heterojunction cells (heterojunction diodes) account an ideality factor greater than 2, *eg* as the result of the recombination at the interface of the heterojunction [21]. At the same time, the lower value $m$ for BB2, along with previous findings, indicates that a lower $CH_4$ content in the gaseous mixture has also an impact on the formation of a better interface between the bulk silicon and the thin SiC layer.

The calculated values can be understood in such way that the samples produced at a lower ratio of methane to silane in their mixture and with denser grid of finger electrodes result in better DC parameters. Low fill factor values (about 0.4) was obviously caused by poor collection of photogenerated carriers and unrealized conventional photovoltaic cell structural components. Typical passivation or antireflection layer applied on silicon carbide could be ZnO or other TCO films.

The standard impedance spectroscopy measurements were performed in order to get an insight on the electrical transport processes in the prepared heterostructures.

Capacitance character of the complex impedance for all samples is demonstrated in Fig. 5. The most convenient fit assumes the series resistance and two parallel $R$-CPE's elements. The constant phase element represents nonlinear capacity, respectively capacity dispersion. It is introduced into the AC equivalent circuit for the structures containing a greater number of structural defects or disorders [22].

The impedance of constant phase element is given as

$$Z_{\mathrm{CPE}} = 1/P(i\omega)^n. \qquad (2)$$

Both CPEs shows exponent $n$ lower than 1 while pure capacitance show exponent $n = 1$. Decreasing $n$ reveals more disordered structure and dispersion of transport processes. The dynamic origin related to multiple trapping systems can be the reason of such behavior. Both, CPE capacitance $P$ and its exponent $n$ depends on the applied DC bias, see Figs. 7–9. Near capacitive behavior ($n$ is closed to 1 and voltage independent), as it is clearly recognized in Fig. 9, was observed for second CPE element in AC equivalent circuit for both samples. The capacity of the structure in forward direction is closely related to the minority charge carriers and thus recombination rate. Second CPE capacitance consistently increases with increasing bias voltages for both samples as one can recognize in Fig. 8. CPE capacitance $P_1$ decreases for both BB1 and BB2 samples (Fig. 7) while CPE capacitance $P_2$ increases when DC bias is increased (Fig. 6). The injection of minority carriers results in diffusion (dynamic) CPE capacitance increase at higher forward bias as typical for this type of structure [23]. Similarly, as in the case of capacitances, the two types of resistances are taken into account in the AC equivalent circuit. In terms of obtained resistance, Fig. 6 shows behavior of both samples. The voltage dependence of resistance indicates two areas dependent on voltage. Two types of resistances are related to shunt and dynamic resistance. The resistance $R_2$ is ascribed to space charge region of the junction and of course it is dependent on the applied bias. Its value under forward direction is much lower than that one under reverse bias. The higher its value, the better the diode interface [24]. At higher forward voltages the transport process is governed by series resistance.

## 4 Conclusion

A thin layers of hydrogenated boron doped amorphous silicon carbide intended for the use as an active part of heterojunction solar cell was studied. Prepared structures represent the basis for further heterojunction solar cells. The investigation was based on the results of DC electrical characterization and AC impedance spectroscopy. Electric PV parameters were obtained from DC measurements. AC equivalent circuit was obtained by analyzing the impedance data at broad frequency range. The physical significance of the individual AC equivalent circuit elements and its relation to the electrical transport processes has been explained. Optimization of deposition process, mainly $CH_4$ gas flow, lead to significant improvement — increase of short circuit current and generated power in the case of BB2 sample. Nevertheless, further research and optimization of deposition technique, as well as structural improvements, like AR coating and photon management, are required in order to produce efficient heterojunction solar cells.

*Acknowledgements*

This work was supported by the Slovak Research and Development Agency (APVV) under the contracts APVV-15-0326, APVV-0443-12. This work was supported by the Scientific Grant Agency of the Ministry of Education of the Slovak Republic and of the Slovak Academy of Sciences under Project VEGA1/0651/16. This contribution is also the result of the project implementation: National Centre for Research and Application of Renewable Energy Sources (ITMS: 26240120016), supported by the Research & Development Operational Programme funded by the EU.

## References

[1] D. A. Anderson and W. E. Kspear, "Electrical and Optical Properties of Amorphous Silicon Carbide, Silicon Nitride and Germanium Carbide Prepared by Glow Discharge Technique", *Philos. Mag. B* vol. 35, 1977, pp. 113–131.

[2] P. P. Dey and A. Khare, "Effect of Substrate Temperature on Structural and Linear and Nonlinear Optical Properties of Nanostructured PLD a-SiC thin films", *Materials Research Bulletin* vol. 84, 2016, pp. 105–117.

[3] I. Kleps and A. Angelescu, "LPCVD Amorphous Silicon Carbide Films, Properties and Microelectronics Applications", *J. Phys. IV France* vol. 09 no. 8, 1999, pp. 1115–1122.

[4] G. Monaco, M. Gastaldi, P. Nicolosi, M. G. Pelizzo, E. Gilioli, S. Rampino, F. Bissoli, F. Pattini, S. Agnoli, G. Granozzi and N. Manuzzato, "Silicon Carbide Thin Films for EUV and Soft X-Ray Applications", *The European Physical Journal Special Topics*, vol. 169, no. 1, 2009, pp. 159–165.

[5] A. C. Barnes, C. A. Zorman and P. X. L. Feng, "Amorphous Silicon Carbide ($\alpha$-SiC) Thin Square Membranes for Resonant Micromechanical Devices", *Materials Science Forum*, vol. 717-720, 2012, pp. 533–536.

[6] J. Ma, J. Ni, J. Zhang, Z. Huang, G. Hou, X. Chen, X. Zhang, X. Geng and Y. Zhao, "Improvement of Solar Cells Performance by Boron Doped Amorphous Silicon Carbide/Nanocrystalline Silicon Hybrid Window Layers", *Solar Energy Materials and Solar Cells*, vol. 114, 2013, pp. 9–14.

[7] T. Brodic, "Trends and Developing of New Semiconductor Power Devices based on SiC and Diamond Materials", *Journal of Electrical Engineering*, vol. 52, 2001, pp. 105–116.

[8] R. Kosiba, G. Ecke, J, Liday, J, Breza and O. Ambacher, "Auger Depth Profiling and Factor Analysis of Sputter Induced Altered Layers SiC", *Journal of Electrical Engineering*, vol. 54, 2003, pp. 52–56.

[9] P. M. Sarro, "Silicon Carbide as a New MEMS Technology", *Sensors and Actuators*, vol. 82, 2000, pp. 210–218.

[10] M. A. El-khakani, M. Chaker, A. Jean and S. Boily, "Hardness and Young's Modulus of Amorphous a-SiC Thin Films Determined by Nanoindentation and Bulge Tests", *Journal of Materials Research*, vol. 9, 1994, pp. 96–103.

[11] D. Pysch, M. Bivour, M. Hermle and S. W. Glunz, "Amorphous Silicon Carbide Heterojunction Solar Cells on p-Type Substrates", *Thin Solid Films*, vol. 519, no. 8, 2011, pp. 2550–2554.

[12] S. Janz, S. Reber and S. W. Glunz, "Amorphous SiC: Applications for Silicon Solar Cells", *Proceedings of the 21st EUPVSEC*, Dresden, 2006, p. 660.

[13] W. Lisheng, C. Yu and A. Fengxiang, "Simulation of High Efficiency Heterojunction Solar Cells with AFORS-HET", *Journal of Physics: Conference Series*, vol. 276, no. 1, 2011, 12177.

[14] M. Kubon, E. Boehmer, M. Gastel, F. Siebke, W. Beyer, C. Beneking and H. Wagner, "Solution of the ZnO/p Contact Problem a-Si:H Solar Cells", *Sol. Energy Mater. Sol. Cells*, vol. 485, 1996, pp. 41–42.

[15] R. Ferre, I. Martin, P. Ortega, M. Vetter, M. Garin and R. Alcubilla, "c-Si Surface Passivation for Photovoltaic Applications by Means of Antireflective Amorphous Silicon Carbide Layers", *Electron Devices, Spanish Conference on Electron Devices*, 2007, pp. 238–241.

[16] S. W. Glunz, E. Schneiderlöchner, D. Kray, A. Grohe, M. Hermle, H. Kampwerth, R. Preu and G. P. Willeke, "Laser-Fired Contact Silicon Solar Cells on p and n Substrates", *Proc. of the 19th EU-PVSEC*, 2004, pp. 408–411.

[17] S. Janz, S. Reber, H. Habenicht, H. Lautenschlager and C. Schetter, "Processing of c-Si Thin-Film Solar Cells on Ceramic Substrate with Conductive SiC Diffusion Barrier Layer", *Proceedings of the 4th WCPEC*, Hawaii, 2006, pp. 1403–1406.

[18] M. Perný, V. Šály and M. Váry, "Optimization of Technology of Amorphous Silicon Carbide Thin Layers", *ELOSYS. Elektrotechnika, informatika a telekomunikácie* 2015 [elektronic source], Trenčín, Slovakia, 13-15 October 2015, Bratislava: Nakladateľstvo STU v Bratislave, 2015, CD-ROM, pp. 116–120.

[19] V. šály, M. Perný, J. Packa, F. Janíček, M. Váry, M. Mikolášek and J. Huran, "AC and DC Response of Heterojunction a-SiC/c-Si for PV Application", *EPE 2017: 18th International scientific conference on electric power engineering,* Kouty nad Desnou, Czech Republic, May 17-19, 2017. Technical University of Ostrava, 2017, pp. 623–626.

[20] C. Gabriel, "PV Cells Electrical Parameters Measurement", *Journal of Electrical Engineering*, vol. 68, no. 7, 2017, pp. 74–77.

[21] M. Elnaby, A. Zekry, F. Elakkad and H. F. Ragai, "Dependence of Dark Current on Zine Concentration Znx $Cd_{1-x}$ S/Zn Te Heterojunctions", *Solar Energy Materials and Solar Cells*, vol. 29, 1993.

[22] J. Bisquert and F. Fabregat-santiago, "Impedance Spectroscopy: A General Introduction and Application to Dye-Sensitized Solar Cells", *Dye-sensitized Solar Cells*, K. Kalyanasundaram ed., CRC Press, 2010.

[23] S. M. Sze, "Physics of Semiconductor Devices", second ed., Wiley, NewYork, 1981.

[24] L. Sunhwa, P. P. Seungman, ?. Jinjoo, K. Youngkuk, P. Hyeongsik, J. Juyeun, S. Chonghoon, L. Youn-jung, B. Seungsin, K. Minbum, J. Junhee and Y. Junsin, "Impedance Spectroscopic Study of p-i-n Type a-Si Solar Cell by Doping Variation of p-Type Layer", *International Journal of Photoenergy*, 2012 Article ID 767248.

Received 5 November 2017